ACS OMEGA

Open Access

http://pubs.acs.org/journal/acsodf

Article

Development of an Albumin-Masked mutPD-1Ig as a Tumor Lesion-Selective Immune Checkpoint Inhibitor

Chien-Yu Chou,[▽] Zhi-Qin Li,[▽] Hsiao-Chen Huang, Chung-Heng Hung, Shun-Long Weng,* and Shey-Cherng Tzou*

Cite This: *ACS Omega* 2023, 8, 40911−40920

Read Online

ACCESS | Metrics & More | Article Recommendations | Supporting Information

ABSTRACT: The antitumor effects elicited by immune checkpoint inhibitors (ICIs) have transformed cancer treatments. However, severe immune-related adverse events (irAEs) resulting from these treatments have restricted the application of ICIs. To overcome the adverse events, we developed a tumor lesion-selective pro-PD-1Ig that is activated by proteases overexpressed in tumors. We genetically linked albumin to the N-terminus of a modified PD-1Ig (termed mutPD-1Ig hereafter) via an MMP substrate sequence to form Alb-hinge-mutPD-1Ig. We demonstrate that the binding activity of nondigested Alb-hinge-mutPD-1Ig is approximately 11-folds lower than mutPD-1Ig. However, digestion by type IV collagenase restored the binding activity of Alb-hinge-mutPD-1Ig to a level comparable to that of native mutPD-1Ig. In order to enhance the masking efficiency of Alb-mutPD-1Ig, we simulated the effects of diverse MMP substrate linkers for connecting albumin and PD-1 at various starting positions by bioinformatics tools. Our validation experiments indicate Alb-hinge-mutPD-1Ig displayed the best masking efficiency among all simulated constructs. Our study suggests that albumin may be best applicable to mask a target protein whose binding motif is centralized and in the proximity of the N-terminus of the protein.

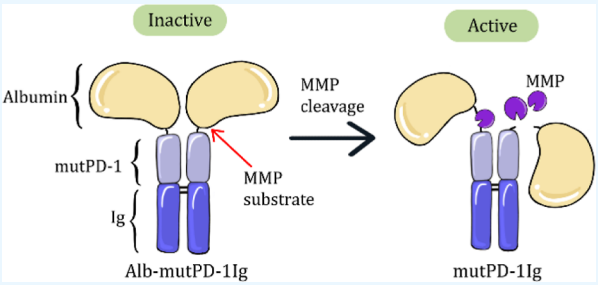

INTRODUCTION

Programmed cell death 1/programmed cell death 1 ligand 1 (PD-1/PD-L1) are crucial immune checkpoints that down-regulate immune responses.[1] Mechanistically, binding of PD-L1 to PD-1 induces the phosphorylation of the PD-1 cytoplasmic tail that recruits tyrosine phosphatase to dampen the T cell receptor signal transduction pathway.[2,3] Consequently, T cell proliferation[4] and production of cytokines such as interferon-γ[5] are reduced after PD-1 engagement with PD-L1. Inadequate expression of these immune checkpoints contributes to autoimmune diseases,[1] highlighting the importance of the immune checkpoints in maintaining immune homeostasis. Conversely, cancers exploit immune checkpoints to evade immunosurveillance. It is known that several cancers express PD-L1 to engage PD-1 expressed on tumor-infiltrating T cells to suppress their anticancer activity.[6,7] The expression of PD-L1 on cancer cells demonstrates a negative correlation with prognosis, underscoring its implication in cancer progression.[8−10] Therefore, blocking these immune checkpoints is a rational strategy to boost antitumor immunity.

FDA has approved several blocking antibodies against PD-1 or PD-L1 for treating multiple cancers, including non-small cell lung cancer,[11] liver cancer,[12] colorectal cancer,[13] cervical cancer,[14] melanoma,[15] and gastric cancer.[16] PD-1/PD-L1 blocking antibodies have been reported to enhance specific T cell responses against neoantigens released from dead cancer cells, in line with the notion that blockade of PD-1/PD-L1 checkpoint enhances antitumor immunity.[17,18] However, challenges have arisen in the application of PD-1/PD-L1 blocking antibodies. First, PD-1/PD-L1 blocking antibodies are associated with multiple immune-related adverse effects (IrAEs), of which 14% were ≥ grade-3 severity.[19,20] Second, only 20−30% of cancer patients responded to the PD-1/PD-L1 antibody therapies.[21] Thus, not all cancer patients will benefit from PD-1/PD-L1 blocking antibodies, and further developments of efficacious and safe inhibitors to PD-1/PD-L1 are needed.

Directing the action of therapeutic proteins (antibodies and other recombinant proteins) to lesions may improve the therapies by reducing the antigenic sink effect and drug-induced adverse effects. To this end, we have previously developed several inactive pro-proteins unless activated by lesion-associated proteases. In particular, we recently engineered an albumin-masked CTLA4Ig (Alb-CTLA4Ig) as a

Received: August 21, 2023
Accepted: October 9, 2023
Published: October 18, 2023

lesion-selective variant of CTAL4Ig.[22] Alb-CTLA4Ig inhibited joint inflammation as effectively as conventional CTLA4Ig but without suppressing systemic immune responses. A structural simulation revealed that albumin covers a sufficient area to mask the binding activity of CTLA4Ig. Hence, albumin may be a promising strategy for constructing lesion-selective proproteins that are inactive in normal tissue but activated by proteases overexpressed in lesions.

In this study, we aimed to engineer a cancer lesion-selective PD-L1 inhibitor for cancer treatment. PD-1 is structurally similar to CTLA4, both of which are grouped in the CD28 receptor family of the immunoglobulin superfamily (IgSF).[23,24] In addition, several matrix metalloproteinases (MMPs) are overexpressed in the tumor microenvironment.[25−27] Based on our experience with Alb-CTLA4Ig, we genetically linked albumin to the N-terminus of a modified PD-1Ig (mutPD-1Ig) through a substrate sequence of MMP2/9 (type IV collagenase) to form Alb-mutPD-1Ig. Albumin can be cleaved and removed by MMP2/9 to restore mutPD-1Ig in the tumor microenvironment (Figure 1). We designed and tested the

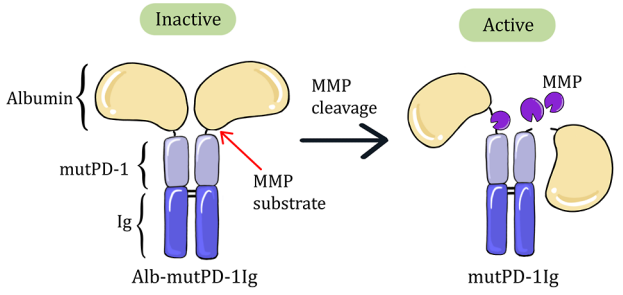

Figure 1. Strategy of cancer lesion-selective Alb-mutPD-1Ig. Albumin is linked to the N-terminus of mutPD-1Ig by a matrix metalloproteinase (MMP) substrate sequence. Albumin masks can be removed to restore the binding activity of mutPD-1Ig by MMPs overexpressed in the tumor microenvironment.

binding activities of several Alb-mutPD-1Ig constructs in which albumin was connected to mutPD-1Ig with a series of different linkers. Furthermore, we tested whether the binding activity of Alb-mutPD-1Ig can be restored after MMPs cleavage. Our data indicate that albumin moderately masks the binding activity of mutPD-1Ig.

MATERIALS AND METHODS

Construction of Expressing Vectors of Recombinant Proteins. The coding sequences of human albumin (Alb) and the extracellular domain (ECD) of human PD-1 were custom-synthesized (Genomics, New Taipei, Taiwan). To construct PD-1Ig, we linked the coding sequences of human wild-type PD-1 to the coding sequences of Fc fragments of a human IgG_1 by overlapping PCR.[28] The PD-1Ig sequence was then subcloned into the pLNCX expression vector using ClaI and SfiI restriction sites. A site-directed mutagenesis kit (New England Biolabs, Ipswich, MA, USA) was used to introduce amino substitutions G124S, K131Y, and A132I in PD-1 ECD to generate mutPD-1Ig. To construct Alb-hinge-mutPD-1Ig, the coding sequences of albumin and mutPD-1Ig were linked through the hinge sequence by a second overlapping PCR and subcloned into the pLNCX vector. Similar cloning procedures were used to generate different Alb-linker-mutPD-1Ig constructs. Table S1 lists the primer sets used in the construction of the fusion proteins (Table S1).

Expression and Purification of Recombinant Proteins. ExpiCHO-S cells were cultured in ExpiCHO expression medium (Thermo Fisher Scientific, Waltham, MA, USA) with shaking (120 rpm) in 8% CO_2 at 37 °C. The expression vectors encoding various constructs were transfected into ExpiCHO-S cells using an ExpiFectamine CHO Transfection Kit (Thermo Fisher Scientific) following the manufacturer's manual. Culture supernatants were collected for purification 10 days after transfection.

To the culture supernatants were added 1% tween-20 and 30 mM imidazole and purified by a nickel-chelating column (GE Life Sciences, Malborough, MA, USA) as previously described.[22] Purified proteins were dialyzed against PBS and stored at −80 °C until use. The purity of the recombinant protein was assessed by SDS-PAGE/coomamassie blue staining. The identity of the recombinant proteins was routinely assessed by Western blot using a HRP-conjugated goat antihuman IgG Fcγ (Jackson ImmunoResearch Laboratories, West Grove, PA, USA). In some cases, Alb-mutPD-1Ig was assessed by Western blot using a mouse antihuman PD-1 antibody, followed by an HRP-conjugated goat antimouse IgG Fcγ (Jackson Immunoresearch Laboratories).

Digestion of Recombinant Proteins by IV Collagenases. Four hundred nanograms (400 ng) of recombinant proteins were cleaved with 2 μg of type IV collagenase (Sigma-Aldrich, St. Louis, MO, USA) in 40 μL of TCNB buffer (0.5% Brij-35, 0.1 M $CaCl_2$, 1.5 M NaCl and 0.5 M Tris, pH 7.5) containing 0.1% BSA, 37 °C for 1 h. EDTA was added to a final concentration of 10 mM to stop the digestion. The extent of collagenase cleavage was assessed by Western blot using a HRP-conjugated goat antihuman IgG Fcγ.

Cell-Based Enzyme-Linked Immunosorbent Assay (ELISA). Ninety-six-well ELISA plates were precoated with polylysine (100 μg/mL, 50 μL/well) at room temperature for 5 min and air-dried. H1975 human lung adenocarcinoma cells were added to the plates (5×10^4 cells/well) and incubated for 14 h. Culture medium were removed, and cells were fixed with 5% formalin in PBS for 30 min on ice. The cells were washed with PBS and then blocked nonspecific binding with 5% skim milk in PBST at room temperature for 1 h. Recombinant proteins were diluted with PBS containing 0.1% BSA and added to the plates at room temperature for 1 h, followed by sequential addition of HRP-conjugated goat antihuman IgG Fcγ and TMB substrate (Invitrogen, Carlsbad, CA, USA). The optical density was measured at 450 nm in a microplate reader (Molecular Devices, San Jose, CA, USA). Half-maximal binding (EC_{50}) was calculated after fitting the absorbance against protein concentrations using a four-parameter logistic fit with the GraphPad Prism software (Graph-Pad, San Diego, CA, USA).

Protein-Based ELISA. Human PD-L1 mouse Fc fusion proteins (Sino Biological, Wayne, PA, USA) were coated (0.1 μg/mL, 50 μL/well) to 96-well plates in PBS. The plates were blocked nonspecific binding with 1% BSA in PBST. Recombinant proteins were added to the plates and detected by ELISA procedures as described in "Cell-based enzyme-linked immunosorbent assay (ELISA)" above.

RESULT

Binding Activity of Alb-Hinge-mutPD-1Ig was Moderately Masked. In order to develop a PD-1Ig as a PD-L1

https://doi.org/10.1021/acsomega.3c06216
ACS Omega 2023, 8, 40911−40920

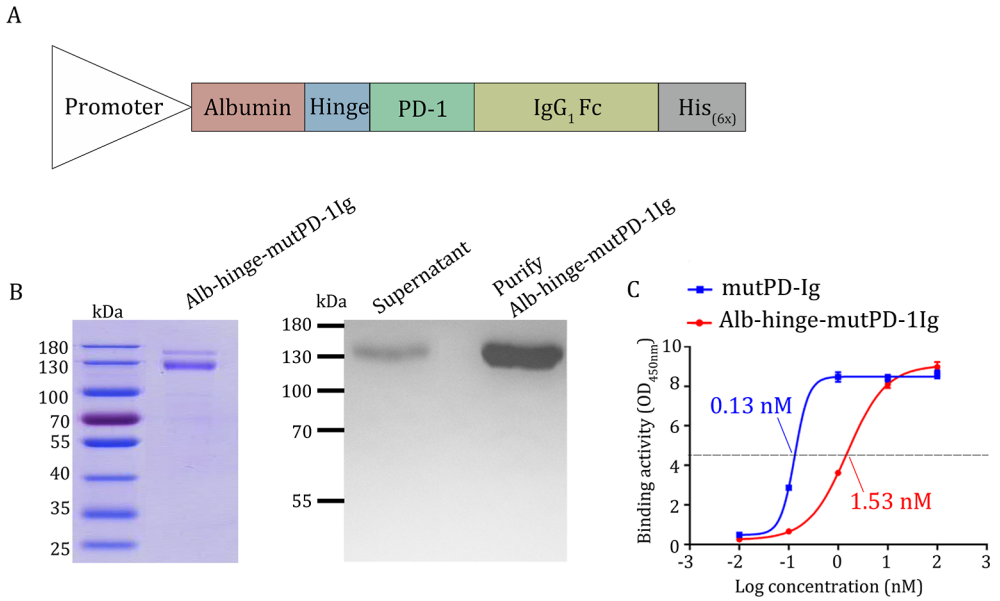

Figure 2. Production and the Masking Effect of Alb-hinge-mutPD-1Ig. (A) Organization of the Alb-hinge-mutPD-1Ig expression vector. $His_{(6x)}$: histidine tag. (B) The purity of Alb-hinge-mutPD-1Ig was assessed by reducing SDS-PAGE/coomassie blue staining (left panel). The identity of the Alb-hinge-mutPD-1Ig was assessed by Western blotting using a HRP-conjugated antihuman Fcγ antibody (right panel). Supernatant: culture supernatants of ExpiCHO-S transiently transfected with Alb-hinge-mutPD-1Ig expression vector. (C) Graded amounts of native mutPD-1Ig (blue curve) and nondigested Alb-hinge-mutPD-1Ig (red curve) were added in a cell-based ELISA where H1975 overexpressing PD-L1 was coated as antigens. The EC_{50} of each protein were indicated by matching colors.

A

Name	Linker sequence	Position on N-terminus of PD-1
Alb-hinge-mutPD-1Ig	CPPCPAPELLGGP	P21
Alb-GPLGVR-mutPD-1Ig	GPLGVR	P21
Alb-PGPLGVR-mutPD-1Ig	PGPLGVR	P21
Alb-hinge-mutPD-1_{P28}Ig	CPPCPAPELLGGP	P28

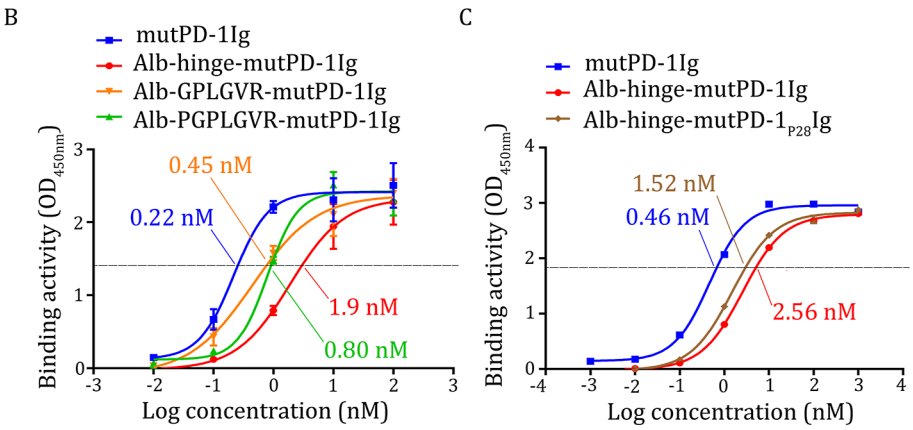

Figure 3. Production and masking effects of Alb-GPLGVR-mutPD-1IIg, Alb-PGPLGVR-mutPD-1Ig, and Alb-hinge-mutPD-1_{P28}Ig. (A) Summary of design of Alb-GPLGVR-mutPD-1IIg, Alb-PGPLGVR-mutPD-1Ig, and Alb-hinge-mutPD-1_{P28}Ig. (B) Graded amounts of mutPD-1Ig (blue curve), Alb-hinge-mutPD-1Ig (red curve), Alb-GPLGVR-mutPD-1Ig (orange curve), and Alb-PGPLGVR-mutPD-1Ig (green curve) were added to the cell-based ELISA. The EC_{50} of each protein were indicated by matching colors. (C) Graded amounts of mutPD-1Ig (blue curve), Alb-hinge-mutPD-1Ig (red curve), and Alb-hinge-mutPD-1_{P28}Ig (brown curve) were added to the cell-based ELISA. The EC_{50} of each protein were indicated by matching colors.

inhibitor, we first constructed an expression vector of PD-1Ig by linking the extracellular domain (P21-R161) (NCBI RefSeq: NP_005009.2) of wild-type human PD-1 and a Fc fragment (Ig) of human IgG[29] (IMGT: J00228). Subsequently, we purified PD-1Ig from the culture supernatants of ExpiCHO-S transiently transfected with the expression vector.

https://doi.org/10.1021/acsomega.3c06216
ACS Omega 2023, 8, 40911−40920

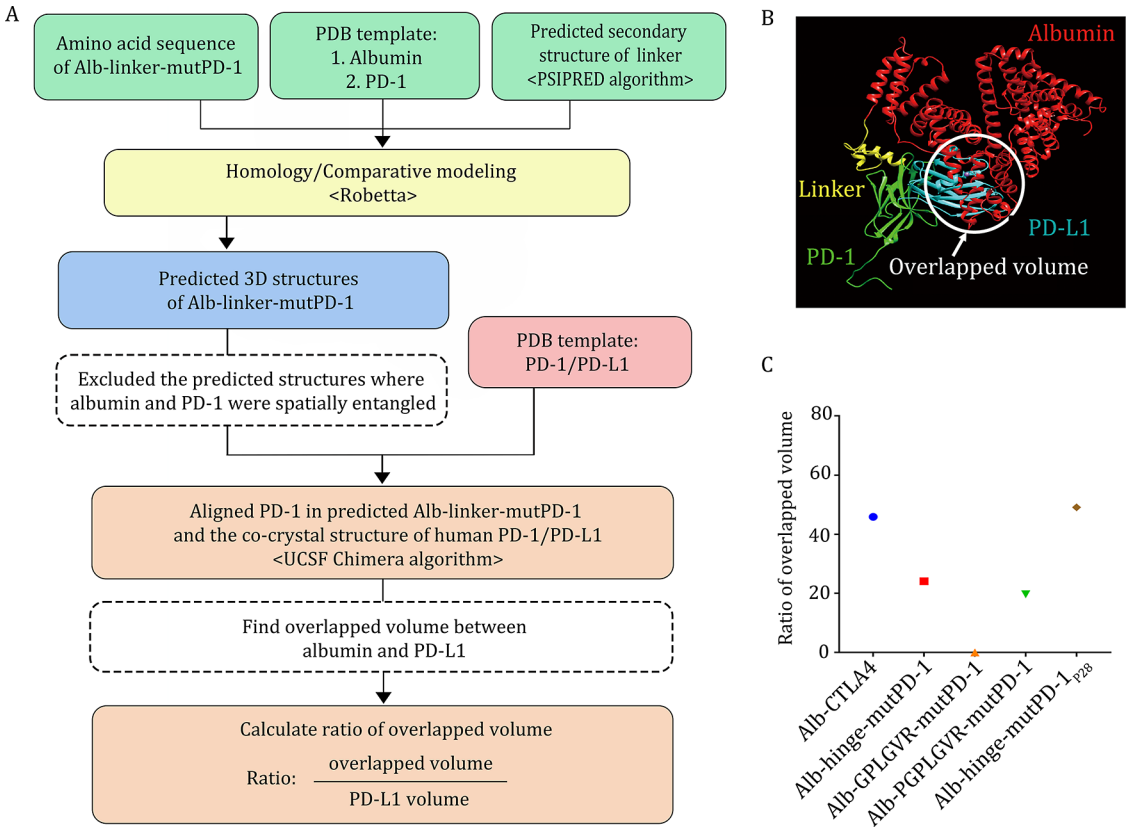

Figure 4. In silico analyses of the masking efficiency of Alb-linkers-PD-1 using bioinformatics analyses. (A) Flowchart of calculating the masking effect of albumin in with predicted structures. (B) Crystal structure of human PD-1/PD-L1 (PDB ID: 4ZQK) and the predicted structure of Alb-hinge-linkers-PD-1 were aligned on PD-1. The extent to which albumin masked the binding of PD-L1 to PD-1 can be determined by considering the region where albumin overlapped with PD-L1 (circle). (C) Estimation of albumin masking effect (expressed as the ratio of overlapped volume) in Alb-hinge-CTLA4, Alb-hinge-mutPD-1 (red), Alb-GPLGVR-mutPD-1 (orange), Alb-PGPLGVR-mutPD-1 (green), and Alb-hinge-mutPD-1_{P28} (brown) using predicted structures. Alb-CTLA4 (blue) was used as a performance reference for the bioinformatics analyses.

However, initial binding tests using cell-based ELISA with PD-L1-expressing cells indicated that wild-type PD-1Ig bound PD-L1 weakly, as 10 nM of wild-type PD-1Ig gave rise to low signal ($OD_{450\ nm}$ = 0.18, Figure S1A), consistent with previous reports indicating that PD-1 binds to PD-L1 with a μM affinity.[23] Similarly, wild-type PD-1Ig bound to PD-L1-expressing cells poorly in flow cytometry (Figure S1B). In order to increase the binding activity of PD-1Ig, we mutated three amino acids at position Gly124, Lys131, Ala132 to Ser, Tyr, and Ile, respectively, in PD-1 ECD following a previous study.[29−32] We produced and purified the mutated PD-1Ig (termed mutPD-1Ig hereafter) from supernatants of ExpiCHO-S transiently transfected with the expression vector encoding mutPD-1Ig. Indeed, the binding activity of mutPD-1Ig increased to 0.1 nM in terms of the EC_{50} (Figure S1C). This mutPD-1Ig was used as a prototype for constructing albumin-masked PD-1Ig fusion proteins in subsequent studies.

In order to develop a tumor lesion-selective mutPD-1Ig, we linked the sequence of human albumin (D25-L609) (NCBI RefSeq: NP_000468.1) to the N-terminus of mutPD-1Ig via a lower hinge/upper CH2 sequence (CPPCPAPELLGGPA) of human IgG (named Alb-hinge-mutPD-1Ig, Figure 2A). We produced and purified Alb-hinge-mutPD-1Ig from supernatants of ExpiCHO-S transiently transfected with the expression vector. Purified Alb-hinge-mutPD-1Ig displayed a monomeric molecular weight of ∼130 kDa under reducing condition (Figure 2B), which is slightly larger than calculated (110.6 kDa), due to glycosylation on PD-1 and IgG Fc.[33,34] The purity of Alb-hinge-mutPD-1Ig after purification was >95% (Figure 2B).

We next tested whether albumin could mask the binding activity of mutPD-1Ig. We analyzed the binding kinetics of Alb-hinge-mutPD-1Ig, using an ELISA in which PD-L1 expressing cells were precoated in the plates as antigens. We found the concentration that gives rise to half-maximal binding signal (EC_{50}) of Alb-hinge-mutPD-1Ig (1.53 nM) is 11.69-fold higher than mutPD-1Ig (0.13 nM) (Figure 2C), indicating albumin masked binding activity of mutPD-1Ig. However, the masking effect of albumin on mutPD-1Ig was moderate.

Construction of Alb-GPLGVR-mutPD-1Ig, Alb-PGPLGVR-mutPD-1Ig, and Alb-Hinge-mutPD-1_{P28}Ig. To test whether the distance between albumin and PD-1Ig affects masking efficacy, we linked albumin and mutPD-1Ig with a shorter MMP2/9 substrate sequence (GPLGVR, Figure 3A). Additionally, we added a proline to the substrate sequence (PGPLGVR, Figure 3A) to introduce an angle between albumin and mutPD-1Ig. These two MMP2/9 substrate sequences lack the cysteine required for disulfide bond formation. Thus, the GPLGVR and PGPLGVR are expected to be flexible linkers.

In Alb-CTLA4Ig, the albumin-hinge sequence is connected to CTLA4 at M38, which is adjacent to the MYPPPY motif. However, in Alb-hinge-mutPD-1Ig, the hinge was connected to PD-1 at P21. Thus, in a third construct, we kept the original

https://doi.org/10.1021/acsomega.3c06216
ACS Omega 2023, 8, 40911−40920

A

No. #	Linker	Position on N-terminus of PD-1
1–1	Hinge	N33
1-2	Hinge	T36
1-3	Hinge+MHV	T36
2-1	Hinge+GSA	P21
2-2	Hinge+GSA	N33
2-3	GSA+Hinge+GSA	P21
2-4	Hinge+GSA+PP	P21
2-5	Hinge+PP+GSA	P21
2-6	$(AP)_7$+Hinge+GSA	N33
3-1	Hinge+AEA	P21
3-2	Hinge+AEA	N33
3-3	AEA+Hinge	P21
3-4	Hinge+AEA+PP	P21
3-5	Hinge+PP+AEA	P21
3-6	$(AP)_7$+Hinge+AEA	N33
3-7	$(AP)_6$+Hinge+AEA	N33
3-8	$(AP)_5$+Hinge+AEA	N33

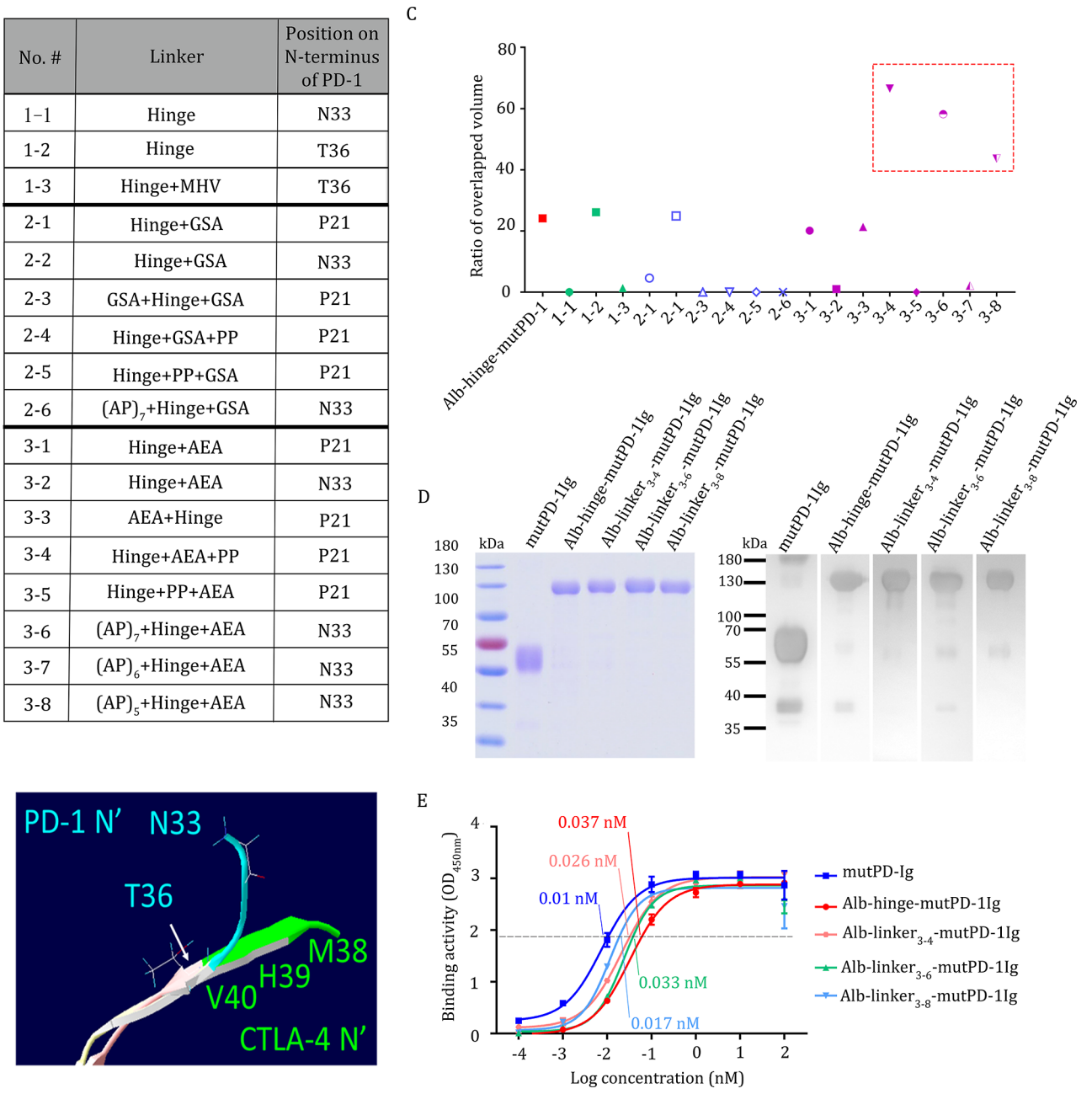

Figure 5. Production and the masking effect of Alb-linker$_{3-4}$-mutPD-1Ig, Alb-linker$_{3-6}$-mutPD-1Ig, and Alb-linker$_{3-8}$-mutPD-1Ig. (A) Summary of the design of Alb-linkers-mutPD-1Ig with different linkers for estimation of the ratio of overlapped volume. (B) Divergence of N-termini of human CTLA-4 and PD-1. (C) The estimation of the albumin masking effect (expressed as ratio of overlapped volume) of the Alb-linkers-mutPD-1Ig with difference linkers. (D) Purity and identity of Alb-linker$_{3-4}$-mutPD-1Ig, Alb-linker$_{3-6}$-mutPD-1Ig, and Alb-linker$_{3-8}$-mutPD-1Ig assessed by reducing SDS-PAGE/coomassie blue staining and Western blotting using a HRP-conjugated antihuman IgG Fcγ antibody. (E) Graded amounts of mutPD-1Ig (blue curve), Alb-hinge-PD-1Ig (red curve), Alb-linker$_{3-4}$-mutPD-1Ig (pink curve), Alb-linker$_{3-6}$-mutPD-1Ig (green curve), and Alb-linker$_{3-8}$-mutPD-1Ig (light blue curve) were added in a protein-based ELISA where purified PD-L1 was coated as an antigen. The EC_{50} of each protein were indicated by matching colors.

hinge sequence but connected to PD-1 at P28, shortening the distance between albumin and mutPD-1Ig (Alb-hinge-mutPD-1$_{P28}$Ig, Figure 3A).

In order to assess the masking effects in Alb-GPLGVR-mutPD-1Ig, Alb-PGPLGVR-mutPD-1Ig, and Alb-hinge-mutPD-1$_{P28}$Ig, we analyzed the binding activity through the cell-based ELISA. We found that GPLGVR/PGPLGVR linkers did not enhance the masking efficiency; the EC_{50} values for GPLGVR-linked and PGPLGVR-linked constructs are 0.45 and 0.8 nM, respectively, compared to 1.9 nM for the original hinge-linked construct (Figure 3B). Similarly, connecting albumin to P28 of mutPD-1 did not enhance the masking efficiency (EC_{50}: 1.52 nM vs 2.56 nM for Alb-hinge-mutPD-1$_{P28}$Ig and Alb-hinge-mutPD-1Ig, respectively, Figure 3C). These data indicate that altering the relative distance of albumin and mutPD-1 by either shortening the linkers or connecting to a deeper amino acid in mutPD-1 did not enhance the masking efficacy by albumin.

Bioinformatics Analyses to Predict the Masking Effects of Alb-Linker-mutPD-1Ig. We considered how

https://doi.org/10.1021/acsomega.3c06216
ACS Omega 2023, 8, 40911−40920

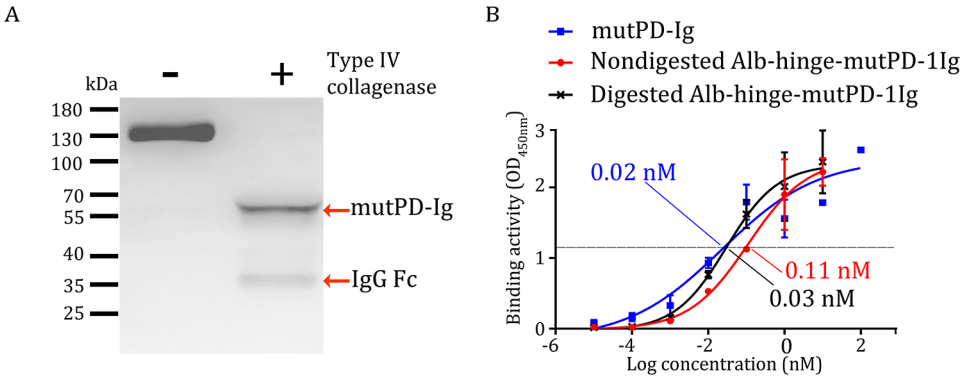

Figure 6. Restoration of binding activity of Alb-hinge-mutPD-1Ig by a type IV collagenase digestion. (A) Digestion of Alb-hinge-mutPD-1Ig by a type IV collagenase for 1 h. The digestions were analyzed by Western blotting using a HRP-conjugated antihuman IgG Fcγ antibody. (B) Graded amounts of native mutPD-1Ig (blue curve), nondigested Alb-hinge-mutPD-1Ig (red curve), and type IV collagenase-digested Alb-hinge-mutPD-1Ig (black curve) were added in a protein-based ELISA where purified PD-L1 was coated as an antigen. The EC_{50} of each protein were indicated by matching colors.

albumin linked to mutPD-1Ig (i.e., linker sequences and connecting amino acid on mutPD-1Ig) could play a major role in determining the masking efficiency of albumin. In order to more systemically and logically design Alb-mutPD-1Ig, we tried bioinformatics tools to model Alb-hinge-mutPD-1 binding to PD-L1 (Figure 4A). First, we used homology modeling to construct the structure of Alb-hinge-mutPD-1 using ROBETTA. For the sake of simplicity, the Ig part of the fusion protein was not included in the prediction. The structure of Alb-hinge-mutPD-1 were predicted using the crystal structures of human albumin (PDB ID: 6JE7), human PD-1 (PDB ID: 2M2D), and the secondary structures of the linkers predicted by the PSIPRED algorithm[35] as templates in the homology modeling.[36] Next, we excluded the predicted structures in which albumin and PD-1 were spatially entangled. Then, we aligned PD-1 in predicted Alb-hinge-mutPD-1 and the cocrystal structure of human PD-1/PD-L1 (PDB ID: 4ZQK,[37]), using the UCSF Chimera algorithm.[38,39] The volume of PD-L1 overlapped by albumin was then calculated (expressed as the ratio of overlapped volume", Figure 4B). As a positive control of the analysis, the volume of CD80 overlapped by albumin in the case of Alb-CTLA4 was calculated. Using this approach, we compared the masking effects of the four Alb-mutPD-1 constructs described in Figure 2. Alb-hinge-mutPD-1 showed a larger overlapped volume (24.1%) than Alb-GPLGVR-mutPD-1 (0%), Alb-PGPLGVR-mutPD-1 (19.7%), but not Alb-hinge-mutPD-1_{P28} (49.1%), in the bioinformatics analysis (Figure 4C). The estimation of the ratio of overlapped volume seemed to agree with the binding test, although more simulation data and the corresponding binding assays could improve the prediction accuracy.

Construction of Alb-linker$_{3-4}$-mutPD-1Ig, Alb-linker$_{3-6}$-mutPD-1Ig, and Alb-linker$_{3-8}$-mutPD-1Ig to Verify the Masking Effects. We used bioinformatics analysis to design the linkage of albumin to mutPD-1Ig. In the first type of design, we used the original hinge sequence between albumin and N33 or T36 of mutPD-1Ig to shorten further the distance between albumin and mutPD-1Ig (Figure 5A). Alternatively, to the hinge sequence were added three amino acids (M38−H39−V40) at the CTLA4 N-terminus, as the overlay of PD-1 and CTLA4 structures indicates two proteins diverge at T36 of PD-1/V40 of CTLA4 (Figure 5B). It was noted that M38−H39−V40 at the N-terminus of CTLA4 is pointed toward the binding site of CTLA4, while the N-terminus of PD-1 (N33−P34−P35) is oriented away from the binding sites of PD-1. The hinge-MHV was linked to mutPD-1 at T36. However, the ratio of overlapped volume calculated from the UCSF Chimera algorithm is either similar (linker 1−2) or lower (linker 1−1 and linker 1−3) than the original Alb-hinge-mutPD-1 (Figure 5C).

In the second and third types of designs, the hinge sequence was combined with different flexible or rigid linkers (Figure 5A). Flexible linkers consist of small amino acids like GSAGSAAGSGEF, offering broader rotation angles (φ and ψ).[40,41] Rigid linkers, such as A$(EAAAK)_2$A, may form α-helix with a fixed angle and length.[42,43] In addition, varying numbers of AP dipeptide repeats $(AP)_n$ were added to the N-terminal of the hinge to introduce different degrees of kinks in the linkers.[41,44] These linkers were connected to P21 and N33 of PD-1. We calculated the ratio of overlapped volume as described above and ranked the potential masking effect of new variants of Alb-hinge-mutPD-1 (Figure 5C). The top three in masking effect are linker 3−4 (66.6%), linker 3−6 (58.2%), and linker 3−8 (43.7%) by the calculation. Therefore, we selected linker 3−4, linker 3−6, and linker 3−8 to link albumin and mutPD-1Ig (named Alb-linker$_{3-4}$-mutPD-1Ig, Alb-linker$_{3-6}$-mutPD-1Ig, and Alb-linker$_{3-8}$-mutPD-1Ig) and produce the recombinant proteins (Figure 5D) for testing the binding activities.

We analyzed the binding kinetics of Alb-linker$_{3-4}$-mutPD-1Ig, Alb-linker$_{3-6}$-mutPD-1Ig, and Alb-linker$_{3-8}$-mutPD-1Ig using a protein-based ELISA where human PD-L1 was coated on the plates as antigen. All albumin-masked mutPD-1Ig proteins displayed a lower binding activity than native mutPD-1Ig, as the binding curves were right-shifted (Figure 5E). Interestingly, protein-based ELISA seemed more sensitive than cell-based ELISA as mutPD-1Ig displayed a lower EC_{50} (0.01 nM) than detected in the cell-based ELISA (~0.2 nM), although a definite conclusion cannot be drawn at the moment due to differences in assay systems. However, the original Alb-hinge-mutPD-1Ig showed the best masking efficacy (EC_{50}: 0.037 nM) compared to Alb-linker$_{3-4}$-mutPD-1Ig (EC_{50}: 0.026 nM), Alb-linker$_{3-6}$-mutPD-1Ig (EC_{50}: 0.033 nM), and Alb-linker$_{3-8}$-mutPD-1Ig (EC_{50}: 0.017 nM). These data indicate that the original Alb-hinge-mutPD-1Ig currently represents the best design to mask the binding activity of mutPD-1Ig using albumin as a masking domain.

https://doi.org/10.1021/acsomega.3c06216
ACS Omega 2023, 8, 40911−40920

Restoration of the Binding Activity of Alb-Hinge-mutPD-1Ig by a Type IV Collagenase Digestion. Finally, we confirmed that Alb-hinge-mutPD-1Ig could be cleaved by type IV collagenase to restore its binding activity to PD-L1. We found type IV collagenase effectively digested Alb-hinge-mutPD-1Ig, as indicated by the reduction of molecular weight (55 kDa), which is equivalent to mutPD-1Ig (Figure 6A). A minor band (4.8%) of 35−40 kDa protein, presumably the IgG Fc fragments, was also noted during the digestion. Furthermore, nondigested Alb-hinge-mutPD-1Ig (EC_{50}: 0.11 nM) showed less binding to PD-L1, whereas type IV collagenase-digested Alb-hinge-mutPD-1Ig showed a comparable binding activity (EC_{50}: 0.03 nM) to the native mutPD-1Ig (EC_{50}: 0.02 nM) (Figure 6B). Thus, the Alb-hinge-mutPD-1Ig cloud can be cleaved by type IV collagenases to restore its binding activity.

DISCUSSION

The current study developed an Alb-hinge-mutPD-1Ig as a potential tumor lesion-selective immune checkpoint inhibitor (ICI) against the PD-1/PD-L1 pathway. Nondigested Alb-hinge-PD-1Ig showed ∼11-fold less binding activity to PD-L1 than type-IV collagenase-digested Alb-hinge-mutPD-1Ig. This 11-fold differential binding activity is in sharp contrast with that of Alb-CTLA4Ig that we have previously developed. We have systemically modified how albumin was linked to mutPD-1Ig without success; several linker sequences or starting positions on mutPD-1 were tested to link albumin and mutPD-1Ig but did not improve the masking efficacy by albumin. Thus far, the original design, where albumin was linked to P21 on mutPD-1 through the hinge sequence (CPPCPAPELLGGPA) showed the best masking efficiency among all constructs.

We seek an explanation as to why albumin can effectively mask CTLA4Ig but not mutPD-1Ig from a structural perspective. We have compared the crystal structures of human CTLA-4 (PDB ID: 3OSK) and PD-1 (PDB ID: 2M2) (Figure S2A), as CTLA4 and PD-1 are both members of CD28 family proteins. The amino acid sequence essential for binding to CD80, MYPPPY (also known as the CDR3-like motif), is located in the FG loop of CTLA-4 that is relatively centralized and close to the N-terminus. However, the binding sites to PD-L1 are dispersedly distributed in the C'CFG strands of PD-1.[45] This suggests that proteins possessing a centralized apical ligand binding motif are more amenable to effective masking by albumin. This reasoning predicts that CD28 would be effectively masked by albumin since CD28 uses the same apical MYPPPY motif (as CTLA4) in its structure to bind CD80/CD86.[46] Inducible costimulator (ICOS) maybe efficiently masked by albumin, since ICOS uses a homologous FDPPPFK motif (amino acids 114−120, located in the FG loop of ICOS) to bind to its ligand ICOS-L.[47] Furthermore, the heavy chains and light chains of antibodies contain three apical complementarity-determining regions (CDRs); blocking any one of the CDRs may significantly interfere with antigen binding. Therefore, albumin could be a useful masking domain for constructing lesion-selective pro-antibodies. Collectively, the future design of pro-proteins using albumin as a masking domain should consider the location and spread of the binding motifs of the target proteins.

PD-1 binds to two natural ligands, PD-L1 and PD-L2. While PD-L1 and PD-L2 suppress T cell activation when bound to PD-1, they differ in their expression patterns. PD-L1 is mainly expressed on hematopoietic cells, while PD-L2 is more widely expressed.[48] In addition, PD-L2 expression is also observed in several cancer types.[49,50] The expression of PD-L2 in cancers negatively correlates with tumor-infiltrating lymphocytes, prognosis, and survival rate.[51−53] Studies on pancreatic ductal adenocarcinomas have found that PD-L2 inhibits $CD8^+$ T cells in tumor tissues and promotes the proliferation of regulatory T cells, thereby establishing an immunosuppressive microenvironment.[54] Whether PD-L1 and PD-L2 play nonredundant roles in promoting cancer immune evasion is unclear. It may be important to determine whether PD-L2 expression is associated with treatment resistance in cancer patients who failed to respond to PD-L1 blocking antibodies. In this regard, mutPD-1Ig may provide a broader application in activating T cells in the tumor microenvironment in that it could block both PD-L1 and PD-L2. On the other hand, on-target, off-tumor toxicity may occur due to the broader binding specificity of mutPD-1Ig. Thus, improving the safety of muPD-1Ig is important for future applications. Our work represents the first attempt to improve the safety of mutPD-1Ig. Further research is needed to increase the masking efficiency.

Our strategy to use albumin as a masking domain in constructing lesion-selective pro-proteins has several advantages. First, albumin masks the binding activity of a target protein by spatial hindrance rather than physical binding to the target protein. Albumin could readily dissociate with the target proteins once the intervening linkers are cleaved by lesion-associated proteases. Other strategies use binder peptides or proteins to the target proteins as masking domains; these binder peptides or proteins could remain firmly bound after cleavage of the linkers. Second, albumin is an endogenous protein in sera,[55] thus albumin is nonimmunogenic. Nonself masking peptides could induce neutralizing antibodies after injected into animals, leading to rapid clearance of the pro-protein. Third, albumin has an extended half-life due to the action of neonatal Fc receptor (FcRn) on the endothelial cells,[56] thus albumin may prolong the existence of the fusion partners in sera. Fourth, albumin is a highly soluble protein, thus albumin may increase the solubility and overall production of the fusion proteins. Lastly, albumin is a well-known carrier for hydrophobic molecules, thus albumin-linked pro-proteins may be further developed into protein−drug complexes. These attributes support the use of albumin as a masking domain for constructing lesion-selective pro-proteins for enhancing therapy and reducing adverse effects.

CONCLUSIONS

We developed Alb-hinge-mutPD-1Ig in which the binding activity of mutPD-1Ig was masked 11-fold by albumin. We show in the in vitro experiments that Alb-hinge-mutPD-1Ig could be cleaved by a type IV collagenase to restore its binding activity. Alb-hinge-mutPD-1Ig currently represents the optimal design in masking the mutPD-1Ig binding activity with albumin. Further research is needed to develop a lesion-selective pro-mutPD-1Ig with a higher masking efficiency. Our study also indicates that albumin may be best applicable to masking a target protein whose binding motif is centralized and in proximity to the N-terminus of the protein.

ASSOCIATED CONTENT

Supporting Information

The Supporting Information is available free of charge at https://pubs.acs.org/doi/10.1021/acsomega.3c06216.

https://doi.org/10.1021/acsomega.3c06216
ACS Omega 2023, 8, 40911−40920

The binding activities of wild-type PD-1Ig and mutPD-1Ig; crystal structures of extracellular domains of CTLA4 and PD-1; and primer list (PDF)

AUTHOR INFORMATION

Corresponding Authors

Shun-Long Weng − *Department of Medicine, MacKay Medical College, New Taipei City 207 Taiwan, Republic Of China; MacKay Junior College of Medicine, Nursing and Management, Taipei City 100-116 Taiwan, Republic Of China; Department of Obstetrics and Gynecology, Hsinchu MacKay Memorial Hospital, Hsinchu City 300 Taiwan, Republic Of China*; Email: 4467@mmh.org.tw

Shey-Cherng Tzou − *Institute of Molecular Medicine and Bioengineering, National Yang Ming Chiao Tung University, Hsin-Chu 300 Taiwan, Republic Of China; Department of Biological Science and Technology and Center for Intelligent Drug Systems and Smart Bio-devices (IDS2B), National Yang Ming Chiao Tung University, Hsin-Chu 300 Taiwan, Republic Of China; Drug Development and Value Creation Research Center, and Department of Biomedical Science and Environmental Biology, Kaohsiung Medical University, Kaohsiung 800-852 Taiwan, Republic Of China*; orcid.org/0000-0002-6620-8571; Email: sctzou@nycu.edu.tw

Authors

Chien-Yu Chou − *Institute of Molecular Medicine and Bioengineering, National Yang Ming Chiao Tung University, Hsin-Chu 300 Taiwan, Republic Of China*

Zhi-Qin Li − *Department of Biological Science and Technology, National Yang Ming Chiao Tung University, Hsin-Chu 300 Taiwan, Republic Of China*

Hsiao-Chen Huang − *Department of Biological Science and Technology, National Yang Ming Chiao Tung University, Hsin-Chu 300 Taiwan, Republic Of China*

Chung-Heng Hung − *Institute of Molecular Medicine and Bioengineering, National Yang Ming Chiao Tung University, Hsin-Chu 300 Taiwan, Republic Of China*

Complete contact information is available at: https://pubs.acs.org/10.1021/acsomega.3c06216

Author Contributions

[▽]C.-Y.C. and Z.-Q.L. contributed equally to this work.

Notes

The authors declare no competing financial interest.

ACKNOWLEDGMENTS

Funding Sources—This study was supported by the research grants to Shey-Cherng Tzou (111-2320-B-A49-021 and 111-2314-B-A49-004) from the National Science and Technology Council, Taiwan, ROC. Shey-Cherng Tzou is supported in part by the joint research project grants sponsored by National Yang Ming Chiao Tung University and Kaohsiung Medical University (NYCUKMU-112-I005), Hsinchu MacKay Memorial Hospital (MMH-HB-10803), and by the "Smart Platform of Dynamic Systems Biology for Therapeutic Development" project from the Featured Areas Research Center Program within the framework of the Higher Education Sprout Project of the National Yang Ming Chiao Tung University and Ministry of Education (MOE), Taiwan, ROC. Founders had no role in the study design, data collection, analysis and interpretation, and writing of the paper. The authors express their gratitude to the funding agencies for their support.

ABBREVIATIONS

ICIs, immune checkpoint inhibitors; irAEs, immune-related adverse events; PD-1, programmed cell death 1; PD-L1, programmed cell death ligand 1; PD-L2, programmed cell death ligand 2; IgSF, immunoglobulin superfamily; MMPs, matrix metalloproteinases; Alb, albumin; ECD, extracellular domain; EC_{50}, the concentration that gives 50% of maximal response

REFERENCES

(1) Ribas, A.; Wolchok, J. D. Cancer immunotherapy using checkpoint blockade. *Science* **2018**, *359* (6382), 1350−1355.

(2) Okazaki, T.; Maeda, A.; Nishimura, H.; Kurosaki, T.; Honjo, T. PD-1 immunoreceptor inhibits B cell receptor-mediated signaling by recruiting src homology 2-domain-containing tyrosine phosphatase 2 to phosphotyrosine. *Proc. Natl. Acad. Sci. U.S.A.* **2001**, *98* (24), 13866−13871.

(3) Ai, L.; Xu, A.; Xu, J. Roles of PD-1/PD-L1 Pathway: Signaling, Cancer, and Beyond. *Adv. Exp. Med. Biol.* **2020**, *1248*, 33−59.

(4) Tumeh, P. C.; Harview, C. L.; Yearley, J. H.; Shintaku, I. P.; Taylor, E. J.; Robert, L.; Chmielowski, B.; Spasic, M.; Henry, G.; Ciobanu, V.; et al. PD-1 blockade induces responses by inhibiting adaptive immune resistance. *Nature* **2014**, *515* (7528), 568−571.

(5) Freeman, G. J.; Long, A. J.; Iwai, Y.; Bourque, K.; Chernova, T.; Nishimura, H.; Fitz, L. J.; Malenkovich, N.; Okazaki, T.; Byrne, M. C.; et al. Engagement of the PD-1 immunoinhibitory receptor by a novel B7 family member leads to negative regulation of lymphocyte activation. *J. Exp. Med.* **2000**, *192* (7), 1027−1034.

(6) Dong, H.; Strome, S. E.; Salomao, D. R.; Tamura, H.; Hirano, F.; Flies, D. B.; Roche, P. C.; Lu, J.; Zhu, G.; Tamada, K.; et al. Tumor-associated B7-H1 promotes T-cell apoptosis: a potential mechanism of immune evasion. *Nat. Med.* **2002**, *8* (8), 793−800.

(7) Dermani, F. K.; Samadi, P.; Rahmani, G.; Kohlan, A. K.; Najafi, R. PD-1/PD-L1 immune checkpoint: Potential target for cancer therapy. *J. Cell. Physiol.* **2019**, *234* (2), 1313−1325.

(8) Gu, L.; Chen, M.; Guo, D.; Zhu, H.; Zhang, W.; Pan, J.; Zhong, X.; Li, X.; Qian, H.; Wang, X. PD-L1 and gastric cancer prognosis: A systematic review and meta-analysis. *PLoS One* **2017**, *12* (8), No. e0182692.

(9) Xu, Y.; Song, G.; Xie, S.; Jiang, W.; Chen, X.; Chu, M.; Hu, X.; Wang, Z. w. The roles of PD-1/PD-L1 in the prognosis and immunotherapy of prostate cancer. *Mol. Ther.* **2021**, *29* (6), 1958−1969.

(10) Xie, M.; Huang, X.; Ye, X.; Qian, W. Prognostic and clinicopathological significance of PD-1/PD-L1 expression in the tumor microenvironment and neoplastic cells for lymphoma. *Int. Immunopharmacol.* **2019**, *77*, 105999.

(11) Rizvi, H.; Sanchez-Vega, F.; La, K.; Chatila, W.; Jonsson, P.; Halpenny, D.; Plodkowski, A.; Long, N.; Sauter, J. L.; Rekhtman, N.; et al. Molecular Determinants of Response to Anti-Programmed Cell Death (PD)-1 and Anti-Programmed Death-Ligand 1 (PD-L1) Blockade in Patients With Non-Small-Cell Lung Cancer Profiled With Targeted Next-Generation Sequencing. *J. Clin. Oncol.* **2018**, *36* (7), 633−641.

(12) Oura, K.; Morishita, A.; Tani, J.; Masaki, T. Tumor Immune Microenvironment and Immunosuppressive Therapy in Hepatocellular Carcinoma: A Review. *Int. J. Mol. Sci.* **2021**, *22* (11), 5801.

(13) Jin, Z.; Sinicrope, F. A. Mismatch Repair-Deficient Colorectal Cancer: Building on Checkpoint Blockade. *J. Clin. Oncol.* **2022**, *40* (24), 2735−2750.

(14) Kagabu, M.; Nagasawa, T.; Sato, C.; Fukagawa, Y.; Kawamura, H.; Tomabechi, H.; Takemoto, S.; Shoji, T.; Baba, T. Immunotherapy for Uterine Cervical Cancer Using Checkpoint Inhibitors: Future Directions. *Int. J. Mol. Sci.* **2020**, *21* (7), 2335.

https://doi.org/10.1021/acsomega.3c06216
ACS Omega 2023, 8, 40911−40920

(15) Jerby-Arnon, L.; Shah, P.; Cuoco, M. S.; Rodman, C.; Su, M. J.; Melms, J. C.; Leeson, R.; Kanodia, A.; Mei, S.; Lin, J. R.; et al. A Cancer Cell Program Promotes T Cell Exclusion and Resistance to Checkpoint Blockade. *Cell* **2018**, *175* (4), 984−997.e24.
(16) Li, K.; Zhang, A.; Li, X.; Zhang, H.; Zhao, L. Advances in clinical immunotherapy for gastric cancer. *Biochim. Biophys. Acta, Rev. Cancer* **2021**, *1876* (2), 188615.
(17) Xu, F.; Jin, T.; Zhu, Y.; Dai, C. Immune checkpoint therapy in liver cancer. *J. Exp. Clin. Cancer Res.* **2018**, *37* (1), 110.
(18) Dong, Y.; Sun, Q.; Zhang, X. PD-1 and its ligands are important immune checkpoints in cancer. *Oncotarget* **2017**, *8* (2), 2171−2186.
(19) Hofmann, L.; Forschner, A.; Loquai, C.; Goldinger, S. M.; Zimmer, L.; Ugurel, S.; Schmidgen, M. I.; Gutzmer, R.; Utikal, J. S.; Göppner, D.; et al. Cutaneous, gastrointestinal, hepatic, endocrine, and renal side-effects of anti-PD-1 therapy. *Eur. J. Cancer* **2016**, *60*, 190−209.
(20) Topalian, S. L.; Hodi, F. S.; Brahmer, J. R.; Gettinger, S. N.; Smith, D. C.; McDermott, D. F.; Powderly, J. D.; Carvajal, R. D.; Sosman, J. A.; Atkins, M. B.; et al. Safety, activity, and immune correlates of anti-PD-1 antibody in cancer. *N. Engl. J. Med.* **2012**, *366* (26), 2443−2454.
(21) Kalisz, K. R.; Ramaiya, N. H.; Laukamp, K. R.; Gupta, A. Immune Checkpoint Inhibitor Therapy-related Pneumonitis: Patterns and Management. *Radiographics* **2019**, *39* (7), 1923−1937.
(22) Jiang, F. Y.; Zhang, Y. Z.; Tai, Y. H.; Chou, C. Y.; Hsieh, Y. C.; Chang, Y. C.; Huang, H. C.; Li, Z. Q.; Hsieh, Y. C.; Chen, I. J.; et al. A lesion-selective albumin-CTLA4Ig as a safe and effective treatment for collagen-induced arthritis. *Inflamm. Regen.* **2023**, *43* (1), 13.
(23) Cheng, X.; Veverka, V.; Radhakrishnan, A.; Waters, L. C.; Muskett, F. W.; Morgan, S. H.; Huo, J.; Yu, C.; Evans, E. J.; Leslie, A. J.; et al. Structure and interactions of the human programmed cell death 1 receptor. *J. Biol. Chem.* **2013**, *288* (17), 11771−11785.
(24) Zak, K. M.; Grudnik, P.; Magiera, K.; Domling, A.; Dubin, G.; Holak, T. A. Structural Biology of the Immune Checkpoint Receptor PD-1 and Its Ligands PD-L1/PD-L2. *Structure* **2017**, *25* (8), 1163−1174.
(25) Somiari, S. B.; Somiari, R. I.; Heckman, C. M.; Olsen, C. H.; Jordan, R. M.; Russell, S. J.; Shriver, C. D. Circulating MMP2 and MMP9 in breast cancer—potential role in classification of patients into low risk, high risk, benign disease and breast cancer categories. *Int. J. Cancer* **2006**, *119* (6), 1403−1411.
(26) Turpeenniemi-Hujanen, T. Gelatinases (MMP-2 and −9) and their natural inhibitors as prognostic indicators in solid cancers. *Biochimie* **2005**, *87* (3−4), 287−297.
(27) Sun, Z.; Li, R.; Sun, J.; Peng, Y.; Xiao, L.; Zhang, X.; Xu, Y.; Wang, M. Matrix Metalloproteinase Cleavable Nanoparticles for Tumor Microenvironment and Tumor Cell Dual-Targeting Drug Delivery. *ACS Appl. Mater. Interfaces* **2017**, *9* (46), 40614−40627.
(28) Lee, C. J.; Wang, C. C.; Chen, M.; Chuang, K. H.; Cheng, T. L.; Jian, T. Y.; Wang, Y. M.; Huang, T. H.; Liao, K. W.; Tzou, S. C. Development of an inflammatory tissue-selective chimeric TNF receptor. *Cytokine* **2019**, *113*, 340−346.
(29) Maute, R. L.; Gordon, S. R.; Mayer, A. T.; McCracken, M. N.; Natarajan, A.; Ring, N. G.; Kimura, R.; Tsai, J. M.; Manglik, A.; Kruse, A. C.; et al. Engineering high-affinity PD-1 variants for optimized immunotherapy and immuno-PET imaging. *Proc. Natl. Acad. Sci. U.S.A.* **2015**, *112* (47), No. E6506.
(30) Pascolutti, R.; Sun, X.; Kao, J.; Maute, R. L.; Ring, A. M.; Bowman, G. R.; Kruse, A. Structure and Dynamics of PD-L1 and an Ultra-High-Affinity PD-1 Receptor Mutant. *Structure* **2016**, *24* (10), 1719−1728.
(31) Lazar-Molnar, E.; Scandiuzzi, L.; Basu, I.; Quinn, T.; Sylvestre, E.; Palmieri, E.; Ramagopal, U. A.; Nathenson, S. G.; Guha, C.; Almo, S. C. Structure-guided development of a high-affinity human Programmed Cell Death-1: Implications for tumor immunotherapy. *EBioMedicine* **2017**, *17*, 30−44.
(32) Li, Y.; Liang, Z.; Tian, Y.; Cai, W.; Weng, Z.; Chen, L.; Zhang, H.; Bao, Y.; Zheng, H.; Zeng, S.; et al. High-affinity PD-1 molecules deliver improved interaction with PD-L1 and PD-L2. *Cancer Sci.* **2018**, *109* (8), 2435−2445.
(33) Agata, Y.; Kawasaki, A.; Nishimura, H.; Ishida, Y.; Tsubat, T.; Yagita, H.; Honjo, T. Expression of the PD-1 antigen on the surface of stimulated mouse T and B lymphocytes. *Int. Immunol.* **1996**, *8* (5), 765−772.
(34) Wright, A.; Morrison, S. L. Effect of glycosylation on antibody function: implications for genetic engineering. *Trends Biotechnol.* **1997**, *15* (1), 26−32.
(35) Bryson, K.; McGuffin, L. J.; Marsden, R. L.; Ward, J. J.; Sodhi, J. S.; Jones, D. T. Protein structure prediction servers at University College London. *Nucleic Acids Res.* **2005**, *33*, W36.
(36) Jones, D. T. Protein secondary structure prediction based on position-specific scoring matrices 1 1Edited by G. Von Heijne. *J. Mol. Biol.* **1999**, *292* (2), 195−202.
(37) Zak, K. M.; Kitel, R.; Przetocka, S.; Golik, P.; Guzik, K.; Musielak, B.; Dömling, A.; Dubin, G.; Holak, T. A. Structure of the Complex of Human Programmed Death 1, PD-1, and Its Ligand PD-L1. *Structure* **2015**, *23* (12), 2341−2348.
(38) Pettersen, E. F.; Goddard, T. D.; Huang, C. C.; Couch, G. S.; Greenblatt, D. M.; Meng, E. C.; Ferrin, T. E. UCSF Chimera−a visualization system for exploratory research and analysis. *J. Comput. Chem.* **2004**, *25* (13), 1605−1612.
(39) Goddard, T. D.; Huang, C. C.; Ferrin, T. E. Software extensions to UCSF chimera for interactive visualization of large molecular assemblies. *Structure* **2005**, *13* (3), 473−482.
(40) Waldo, G. S.; Standish, B. M.; Berendzen, J.; Terwilliger, T. C. Rapid protein-folding assay using green fluorescent protein. *Nat. Biotechnol.* **1999**, *17* (7), 691−695.
(41) Chen, X.; Zaro, J. L.; Shen, W. C. Fusion protein linkers: property, design and functionality. *Adv. Drug Deliv. Rev.* **2013**, *65* (10), 1357−1369.
(42) Arai, R.; Ueda, H.; Kitayama, A.; Kamiya, N.; Nagamune, T. Design of the linkers which effectively separate domains of a bifunctional fusion protein. *Protein Eng.* **2001**, *14* (8), 529−532.
(43) Arai, R.; Wriggers, W.; Nishikawa, Y.; Nagamune, T.; Fujisawa, T. Conformations of variably linked chimeric proteins evaluated by synchrotron X-ray small-angle scattering. *Proteins* **2004**, *57* (4), 829−838.
(44) Bhandari, D. G.; Levine, B. A.; Trayer, I. P.; Yeadon, M. E. 1H-NMR study of mobility and conformational constraints within the proline-rich N-terminal of the LC1 alkali light chain of skeletal myosin. Correlation with similar segments in other protein systems. *Eur. J. Biochem.* **1986**, *160* (2), 349−356.
(45) Yu, C.; Sonnen, A. F.; George, R.; Dessailly, B. H.; Stagg, L. J.; Evans, E. J.; Orengo, C. A.; Stuart, D. I.; Ladbury, J. E.; Ikemizu, S.; et al. Rigid-body ligand recognition drives cytotoxic T-lymphocyte antigen 4 (CTLA-4) receptor triggering. *J. Biol. Chem.* **2011**, *286* (8), 6685−6696.
(46) Evans, E. J.; Esnouf, R. M.; Manso-Sancho, R.; Gilbert, R. J.; James, J. R.; Yu, C.; Fennelly, J. A.; Vowles, C.; Hanke, T.; Walse, B.; et al. Crystal structure of a soluble CD28-Fab complex. *Nat. Immunol.* **2005**, *6* (3), 271−279.
(47) Rujas, E.; Cui, H.; Sicard, T.; Semesi, A.; Julien, J. P. Structural characterization of the ICOS/ICOS-L immune complex reveals high molecular mimicry by therapeutic antibodies. *Nat. Commun.* **2020**, *11* (1), 5066.
(48) Wang, Y.; Du, J.; Gao, Z.; Sun, H.; Mei, M.; Wang, Y.; Ren, Y.; Zhou, X. Evolving landscape of PD-L2: bring new light to checkpoint immunotherapy. *Br. J. Cancer* **2023**, *128* (7), 1196−1207.
(49) Yearley, J. H.; Gibson, C.; Yu, N.; Moon, C.; Murphy, E.; Juco, J.; Lunceford, J.; Cheng, J.; Chow, L. Q.; Seiwert, T. Y.; et al. PD-L2 Expression in Human Tumors: Relevance to Anti-PD-1 Therapy in Cancer. *Clin. Cancer Res.* **2017**, *23* (12), 3158−3167.
(50) Shin, S. J.; Jeon, Y. K.; Kim, P. J.; Cho, Y. M.; Koh, J.; Chung, D. H.; Go, H. Clinicopathologic Analysis of PD-L1 and PD-L2 Expression in Renal Cell Carcinoma: Association with Oncogenic Proteins Status. *Ann. Surg Oncol.* **2016**, *23* (2), 694−702.

https://doi.org/10.1021/acsomega.3c06216
ACS Omega 2023, 8, 40911−40920

(51) Sumitomo, R.; Huang, C. L.; Fujita, M.; Cho, H.; Date, H. Differential expression of PD-L1 and PD-L2 is associated with the tumor microenvironment of TILs and M2 TAMs and tumor differentiation in non-small cell lung cancer. *Oncol. Rep.* **2022**, *47* (4), 73.
(52) Okadome, K.; Baba, Y.; Nomoto, D.; Yagi, T.; Kalikawe, R.; Harada, K.; Hiyoshi, Y.; Nagai, Y.; Ishimoto, T.; Iwatsuki, M.; et al. Prognostic and clinical impact of PD-L2 and PD-L1 expression in a cohort of 437 oesophageal cancers. *Br. J. Cancer* **2020**, *122* (10), 1535−1543.
(53) Zhang, Y.; Xu, J.; Hua, J.; Liu, J.; Liang, C.; Meng, Q.; Wei, M.; Zhang, B.; Yu, X.; Shi, S. A PD-L2-based immune marker signature helps to predict survival in resected pancreatic ductal adenocarcinoma. *J. Immunother. Cancer.* **2019**, *7* (1), 233.
(54) Goulart, M. R.; Stasinos, K.; Fincham, R. E. A.; Delvecchio, F. R.; Kocher, H. M. T cells in pancreatic cancer stroma. *World J. Gastroenterol.* **2021**, *27* (46), 7956−7968.
(55) Belinskaia, D. A.; Voronina, P. A.; Shmurak, V. I.; Jenkins, R. O.; Goncharov, N. V. Serum Albumin in Health and Disease: Esterase, Antioxidant, Transporting and Signaling Properties. *Int. J. Mol. Sci.* **2021**, *22* (19), 10318.
(56) Andersen, J. T.; Dalhus, B.; Viuff, D.; Ravn, B. T.; Gunnarsen, K. S.; Plumridge, A.; Bunting, K.; Antunes, F.; Williamson, R.; Athwal, S.; et al. Extending serum half-life of albumin by engineering neonatal Fc receptor (FcRn) binding. *J. Biol. Chem.* **2014**, *289* (19), 13492−13502.

https://doi.org/10.1021/acsomega.3c06216
ACS Omega 2023, 8, 40911−40920